

Soil Grouting in the
Mini-Drum Centrifuge

M D Bolton and C Y Chin

CUED/D-Soils/TR266 (1994)

Contents

1 Introduction	1
2 Mk R Mini-Drum Centrifuge	1
2.1 Workings of Mk R Mini-Drum Centrifuge	1
2.2 Grout Injection Equipment	3
2.3 Instrumentation	5
3 Model Preparation	6
4 Stress Profile in the Clay	7
5 Testing Procedure	11
6 Observations	12
Acknowledgements	19
References	10

List of Tables

1 Schedule of Tests	12
-------------------------------	----

List of Figures

1 Elevation of Mk R Mini-Drum Centrifuge	2
2 Cross-section of Mk R Mini-Drum Centrifuge	2
3 Soil Container.	3
4 Grout Injection Equipment	4
5 Aluminium nozzle tip	5
6 Cross-section of soil model	6
7 Plan positions of injection point and PPT's	7
8 Stress changes on rapid unloading of clay specimen	10
9 Theoretical Stress profile of Clay for test CYC 10	10
10 Variation of g-level with depth of 90mm clay specimen for CYC 10 .	11
11 Elevation of Grout ball from Test CYC 8	13
12 Elevation of Grout ball from Test CYC 6	13
13 Exposed section of clay on the 'Horizontal' fracture surface in Test CYC 10	14
14 Cross-section of soil model with fracture details from Test CYC 10 .	14
15 Results from Test CYC 8	16
16 Results from Test CYC 6	17
17 Results from Test CYC 10	18

1 Introduction

The applications of grouting in the construction industry are wide and varied. These include the treatment of ground to facilitate ground water cut-off, pile construction and post-construction applications.

In soft ground tunnel construction, it is well established that a settlement trough develops as the tunnel advances. The damaging effects this has on overlying structures are a cause of great concern. Current construction measures to limit these damages involve the use of grout injected into the ground either prior to tunnelling to improve the strength of the ground or after tunnelling has occurred. In either case, subsidence of the ground is inevitable.

Compensation grouting, through the injection of suitable grouts causing **hydrofracture** at a level between the tunnel and the ground surface ahead of the advancing tunnel face is proposed. Settlements at the ground surface might then be prevented by compensating for ground loss without destabilising the tunnel face. However, the hydrofracture mechanism is not **well** understood and before any confidence can be expressed in its use, this needs to be studied. The Mk R Mini-drum centrifuge was used for the purpose of observing such mechanisms forming in clay under varying stress conditions.

In the first of a series of centrifuge tests, grout in the form of Loctite 241 adhesive is injected into clay blocks. Stress conditions are controlled by varying the **over-consolidation ratios (OCR's)**¹. This technical report will describe the equipment used, the series of tests conducted, and show some of the results obtained.

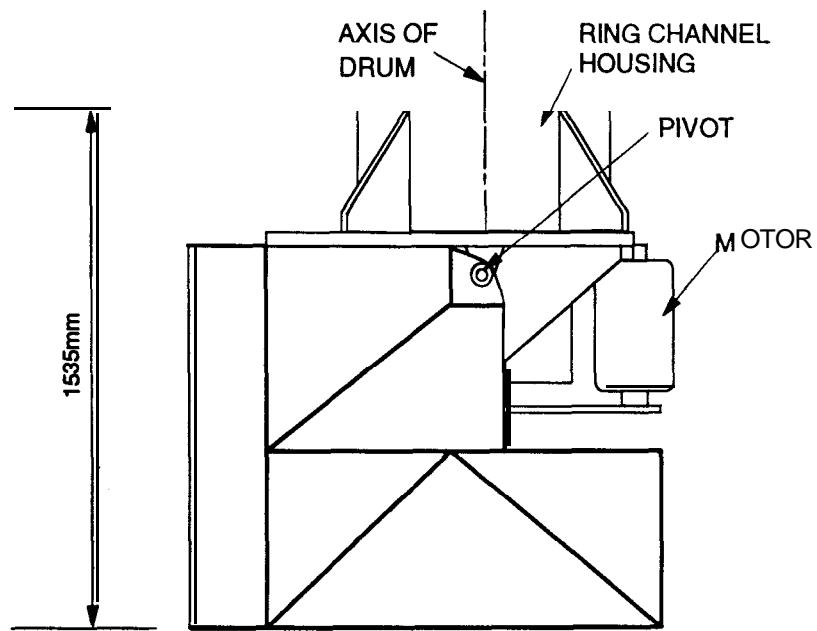
2 Mk R Mini-Drum Centrifuge

2.1 Workings of Mk R Mini-Drum Centrifuge

Figure 1 shows the elevation of the mini-drum with the axis of the drum in the vertical position. The drum can be rotated through 90° with the drive in the horizontal position to facilitate loading and preparation of soil models. The cross-section of the mini-drum centrifuge is shown in Figure 2.

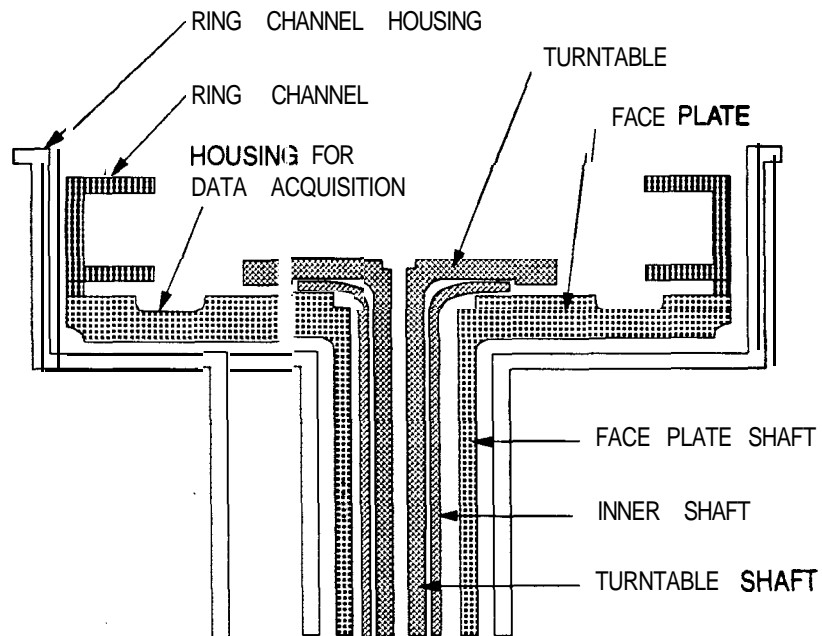
The rotating face plate has two functions. The first is that it supports and rotates the ring channel. Soil containers with internal dimensions 165mm x 165mm x **110mm** deep (Figure 3) are slotted into the ring channel. The second is that it houses two compartments for data acquisition. One compartment contains electronic components such as the multiplexer and programmable gain amplifier, the other houses 16 **Amphenol** bayonet lock connectors for electrical components such as Linear Variable Differential Transducers (**LVDT's**) and load cells.

¹defined here as previous maximum vertical effective stress divided by current vertical effective stress



NOTE : NOT TO SCALE

Figure 1: Elevation of Mk R Mini-Drum Centrifuge



NOTE: NOT TO SCALE

Figure 2: Cross-section of Mk R Mini-Drum Centrifuge

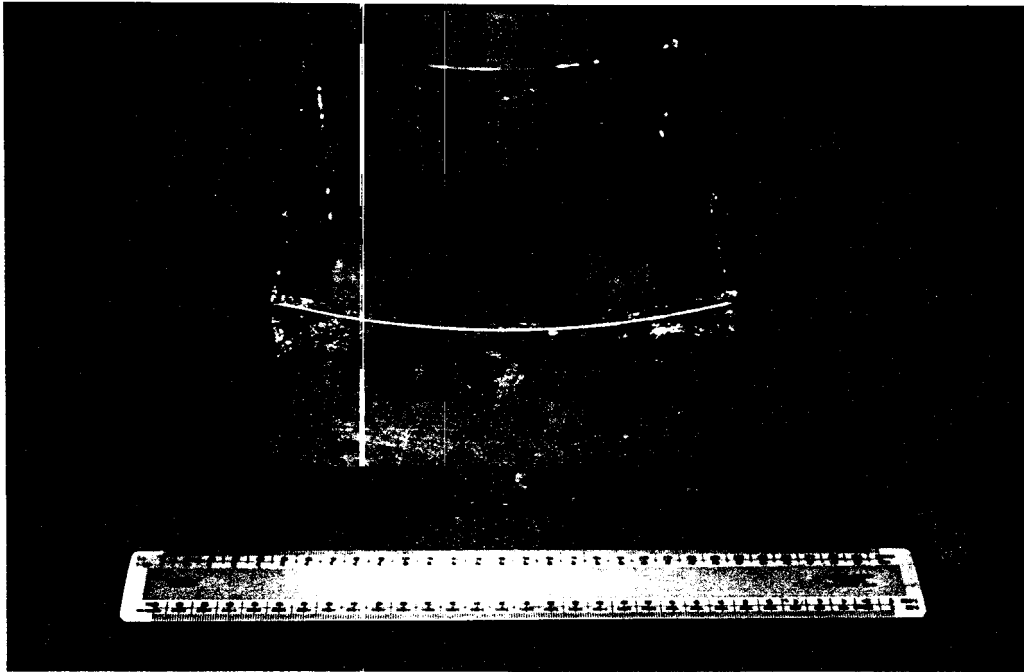


Figure 3: Soil Container

The face plate is permanently connected to the face plate shaft which is rotated via a belt from a brushless AC motor. With the diameter of the face plate at **800mm**, the maximum spindle speed² of **1000rpm** corresponds to 447g at the periphery³.

Concentric to the face plate shaft are two other shafts. The inner shaft is the drive shaft for the turntable and the turntable shaft is a spindle which supports and locates the turntable. The turntable provides a platform 280mm in diameter which supports the grout injection equipment. While in flight, soil models can be viewed with a stroboscope.

2.2 Grout Injection Equipment

Figure 4 shows the grout injection equipment. A 24V D.C. motor drives two pulleys via a belt. This in turn provides linear motion to a screw and pushes a plunger in a medical hypodermic syringe filled with grout. A 5mm OD nylon tube is connected to the syringe. An aluminium nozzle (Figure 5) was developed to be attached to the end of the nylon tube at the point of injection 50mm below the surface of the clay.

Having drawn the required amount of fluid into the syringe, the nylon tube with the aluminium nozzle would be attached to the syringe. A pressure calibrated high-

²speed in revolutions per minute (rpm)

³where lg equals $9.81N/m^2$

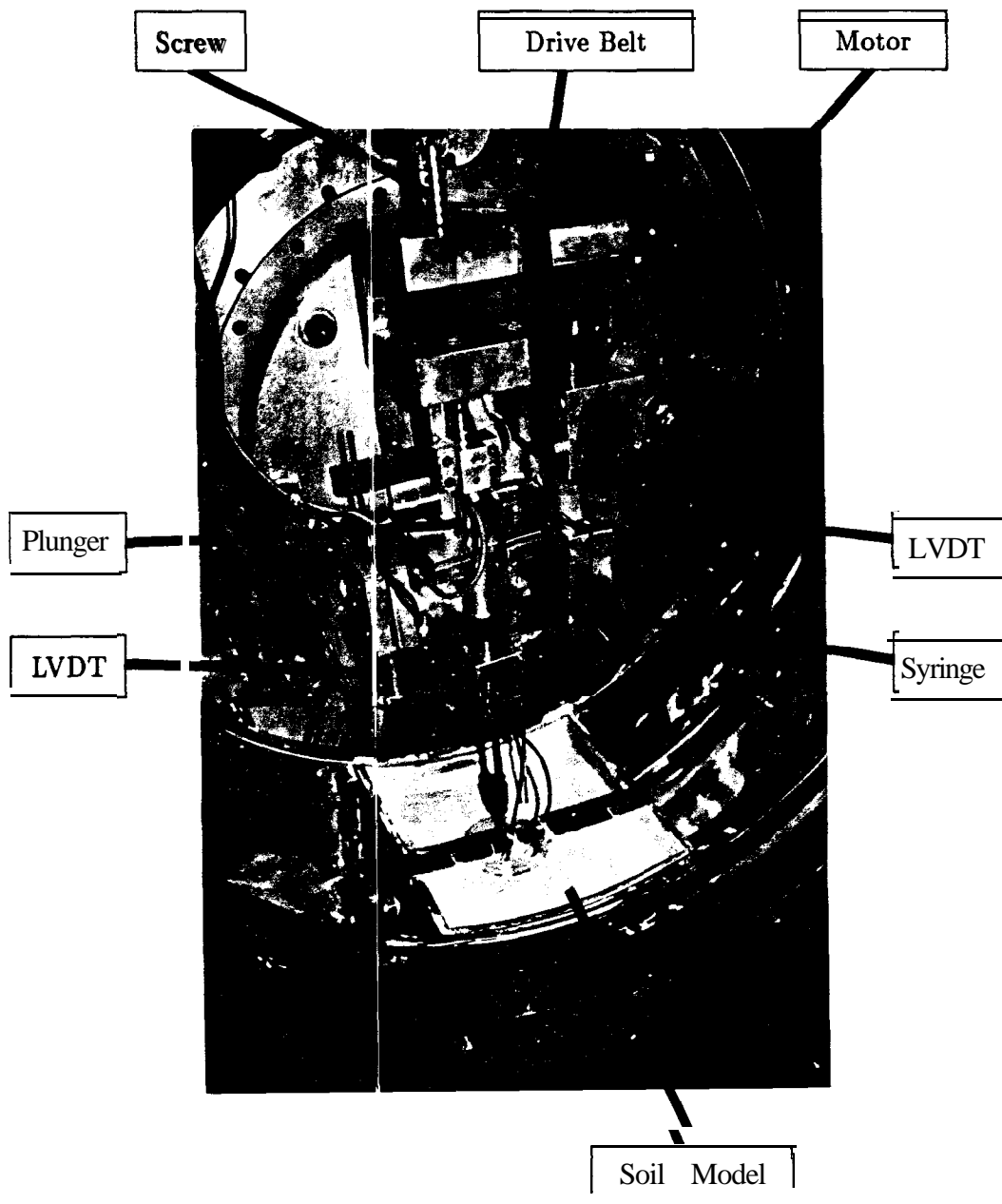


Figure 4: Grout Injection Equipment

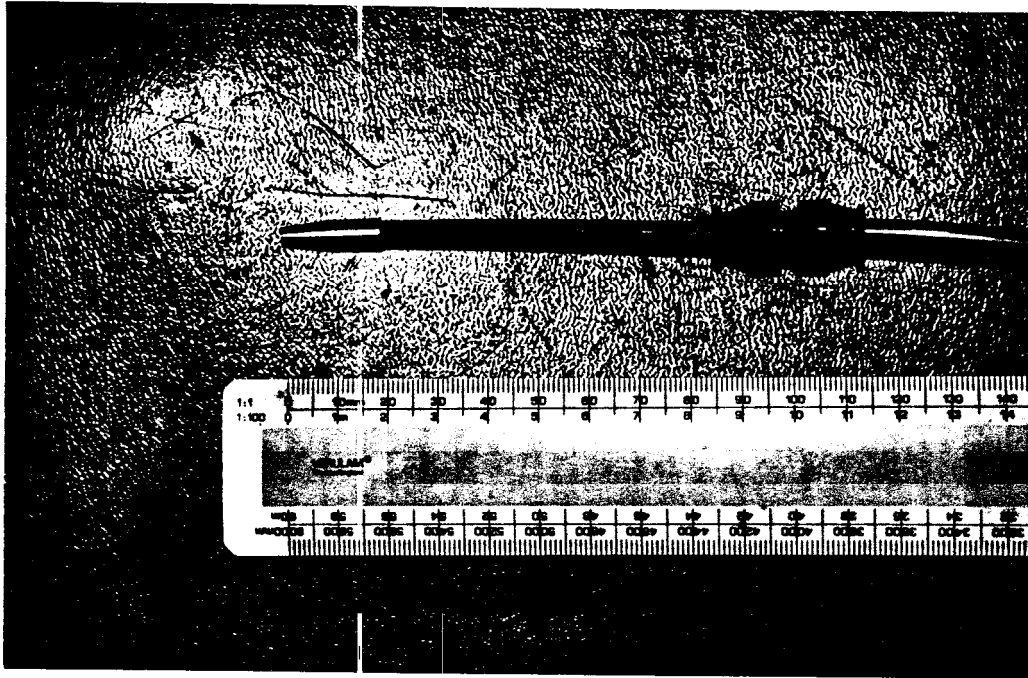


Figure 5: Aluminium nozzle tip

precision rubber ball would be inserted into the aluminium nozzle. The fluid filled syringe would then be mounted onto the equipment and the nozzle introduced into the clay (Figure 6).

When grout injection was required, the motor was switched on and the axially moving plunger would increase the fluid pressure behind the rubber ball. When the force generated by the fluid pressure exceeded the friction holding the ball in the nozzle, the ball would shoot out allowing the grout to penetrate the soil.

Such a system allowing the fluid to be introduced to the soil with a large pressure gradient was found to be necessary for grouting to take place. This technique of introducing grout with a large pressure gradient is similar to the Tube à Manchette technique of grouting commonly found in the construction industry.

2.3 Instrumentation

Instrumentation during centrifuging took the following form :-

1. Two **LVDTs**, one to measure the rate of fluid injection and the other to measure soil heave on the surface of the clay block at the point of injection,
2. Load cells attached to the plunger to provide an indirect measurement of fluid pressure in the syringe,

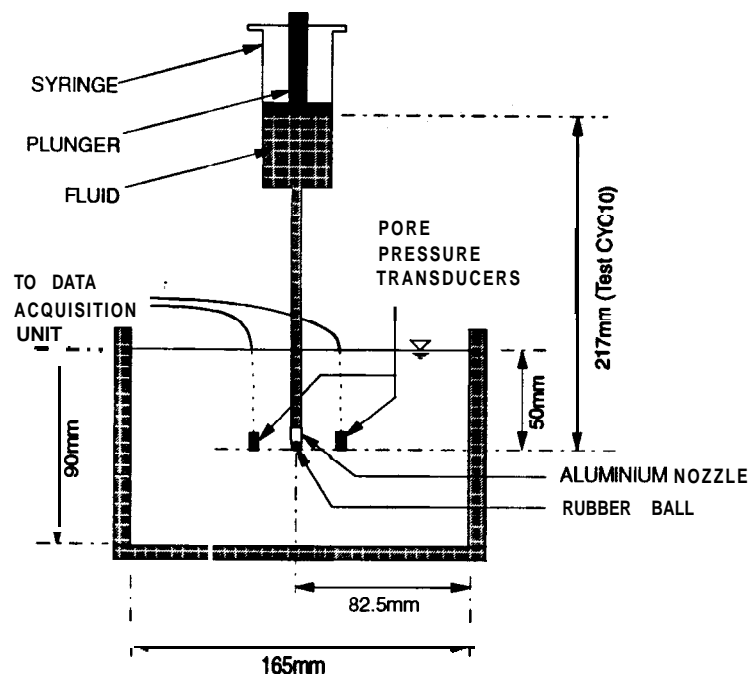


Figure 6: Cross-section of soil model

3. Two **Druck** pore pressure transducers (**PPTs**) placed in the soil at the depth of injection at various radii from the point of injection.

Figure 7 shows the plan locations of the grout injection point and PPT positions. Data during the centrifuge test was acquired via a multiplexer into a data acquisition program, **Labtech** Notebook running in a Dell **486SX 25MHz** IBM compatible computer. During the grout injection, data from the above instrumentation was obtained at **10Hz**.

3 Model Preparation

Speswhite kaolin was used as the soil medium for centrifuge testing. It was prepared by mixing Speswhite kaolin powder with de-ionised water at 120% moisture content under vacuum. Soil containers for centrifuging were positioned in an 850mm diameter consolidometer and kaolin slurry poured into it. The kaolin was consolidated in increments allowing excess pore pressure to dissipate, up to a vertical effective stress of **60kPa**.

At the end of consolidation, the 850mm diameter clay block was jacked up and separated from the consolidometer. Cling film was used to wrap the clay block, minimising any moisture loss from the clay. Before each centrifuge test, the 850mm

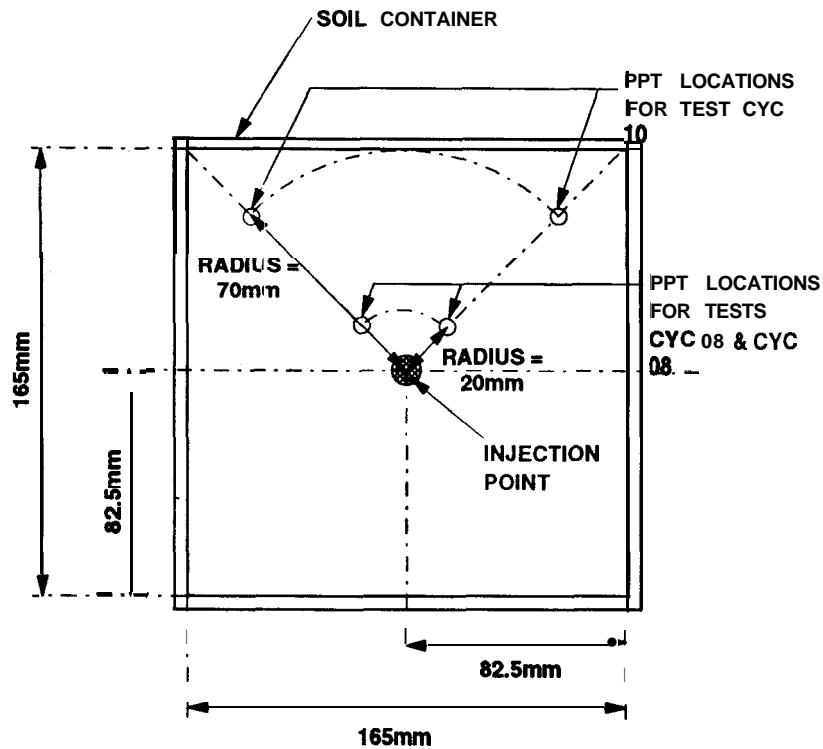


Figure 7: Plan positions of injection point and **PPT's**

diameter clay block would be probed for a soil container of clay and cut out accordingly.

4 Stress Profile in the Clay

It will be useful to consider the stress conditions that exist in the clay block at the consolidation stage and during centrifuging. During consolidation of the clay, pore water in the clay is allowed to drain out. Hence, the pore water pressure, u is zero and the vertical effective stress, σ'_v equals the vertical total stress, σ_v .

Two situations can occur when the consolidometer is unloaded **rapidly**:-

1. No separation of the clay from the sides of the consolidometer,
2. Separation of the clay from the sides of the consolidometer.

Consider the first case when no separation of the clay occurs. This analysis assumes that the clay behaves in an isotropic perfectly elastic manner when unloaded. Hence, for elastic behaviour,

$$\delta v = \frac{\delta p'}{K} \quad (1)$$

where δv is a small change in volume, $\delta p'$ is a small change in mean effective stress and K is the bulk modulus. For undrained loading, δv is zero and hence, the mean normal effective stress must remain constant :-

$$\delta p' = 0 \quad (2)$$

If it is assumed that the sample does not separate from the walls of the **consolidometer** at any stage during the unloading process, then

$$\varepsilon_h = 0 \quad (3)$$

where ε_h is the horizontal strain. Since the volume must remain constant during undrained loading, the vertical strain, ε_v will also be zero. The change in deviator stress is related to shear strain by :

$$\delta q = G(\varepsilon_v - \varepsilon_h) \quad (4)$$

where G is the elastic shear modulus. Since both ε_v and ε_h are zero, δq will also be zero.

$$\delta q = \delta \sigma_v - \delta \sigma_h = 0 \quad (5)$$

thus,

$$\sigma_v - \sigma_h = \sigma_{vo} - \sigma_{ho} \quad (6)$$

and hence

$$\sigma'_v - \sigma'_h = \sigma'_{vo} - \sigma'_{ho} \quad (7)$$

where $\sigma_v, \sigma_h, \sigma'_v, \sigma'_h$ are the vertical and horizontal total and effective stresses at any stage of the unloading. $\sigma_{vo}, \sigma_{ho}, \sigma'_{vo}$ and σ'_{ho} are the corresponding original stresses before unloading commenced.

From Equation (2), we can see that

$$\sigma'_v + 2\sigma'_h = \sigma'_{vo} + 2\sigma'_{ho} \quad (8)$$

From the principle of effective stress, we know that

$$\sigma_{vu} = \sigma'_{vu} + u_u \quad (9)$$

where the subscript u refers to the unloaded state. After unloading, σ_{vu} is zero and hence,

$$\sigma'_{vu} = -u_u \quad (10)$$

Substituting equation (10) into equation (7) gives

$$\sigma'_{hu} = \sigma'_{ho} - \sigma'_{vo} - u_u \quad (11)$$

Substituting equations (10) and (11) into equation (8) gives

$$\begin{aligned} -u_u + 2(\sigma'_{ho} - \sigma'_{vo} - u_u) &= \sigma'_{vo} + 2\sigma'_{ho} \\ -3u_u &= 3\sigma'_{vo} \\ u_u &= -\sigma'_{vo} \end{aligned} \quad (12)$$

This suggests that if no separation takes place, the negative pore pressure after unloading, $-u_u$ is equal to the vertical pressure applied to the clay before unloading, and the effective stress state of the soil is unaffected by unloading.

From equation (7) and substituting q for q' , we obtain

$$\sigma_{vu} - \sigma_{hu} = \sigma'_{vo} - \sigma'_{ho} \quad (13)$$

and since σ_{vu} equals zero,

$$\sigma_{hu} = \sigma'_{ho} - \sigma'_{vo} = \sigma'_{vo}(K_o - 1) \quad (14)$$

where K_o is the coefficient of earth pressure at rest. If K_o is less than unity, the total horizontal stress, σ_{hu} becomes negative, which indicates that a tensile stress acts between the clay and the consolidometer walls. If the pore pressure at the boundary cannot sustain this tensile stress, the sample will separate from the consolidometer wall and the total horizontal stress drops to zero. This leads to the second case where separation of the sample from the consolidometer walls occurs.

On separation, both the total horizontal and vertical stresses (σ_{hu} and σ_{vu}) drop to zero. The sample undergoes shear deformation and the deviator stress, q becomes zero. Effective stress paths observed by Nadarajah (1973) [7] and Foster (1977) [3] in undrained shear tests indicate that the mean normal effective stress, p' remain substantially constant. Making this assumption that p' remains constant when separation occurs, then the negative pore pressure after unloading will equal the mean normal effective stress :-

$$21, = -\frac{\sigma'_{vo}}{3}(1 + 2K_o) \quad (15)$$

Figure 8 shows the stress changes experienced by the clay specimen on rapid unloading for both cases (modified from Mair, 1979 [6]).

In these series of tests, no separation of the clay from the walls of the **consolidometer** was observed. Neither was there any separation observed between the clay and the sides of the soil containers when these containers were cut out from the 850mm diameter block of clay.

With the container of clay secured in the ring channel of the mini-drum, the centrifuge was spun up to the required test speed. Water was then filled in the ring channel to the required depth and pore pressures were monitored using **PPT's** embedded in the clay. When equilibrium conditions were attained, the injection of grout was carried out. Injection of grout took place 50mm below the surface of the

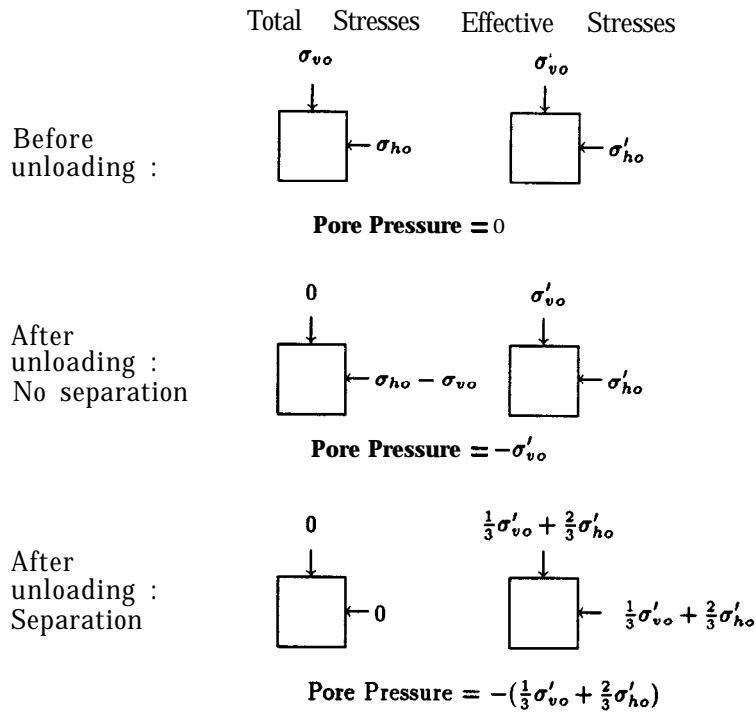


Figure 8: Stress changes on rapid unloading of clay specimen

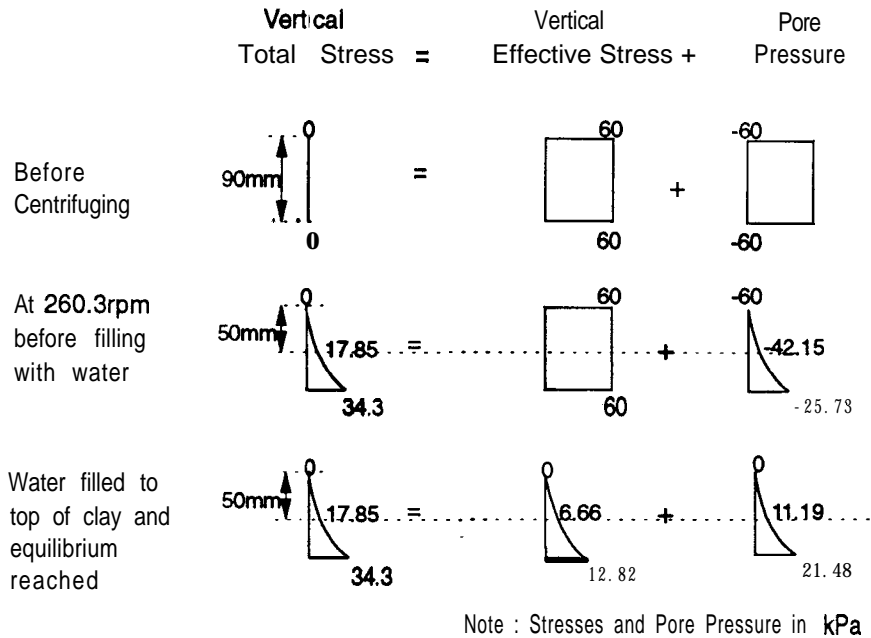


Figure 9: Theoretical Stress profile of Clay for test CYC 10

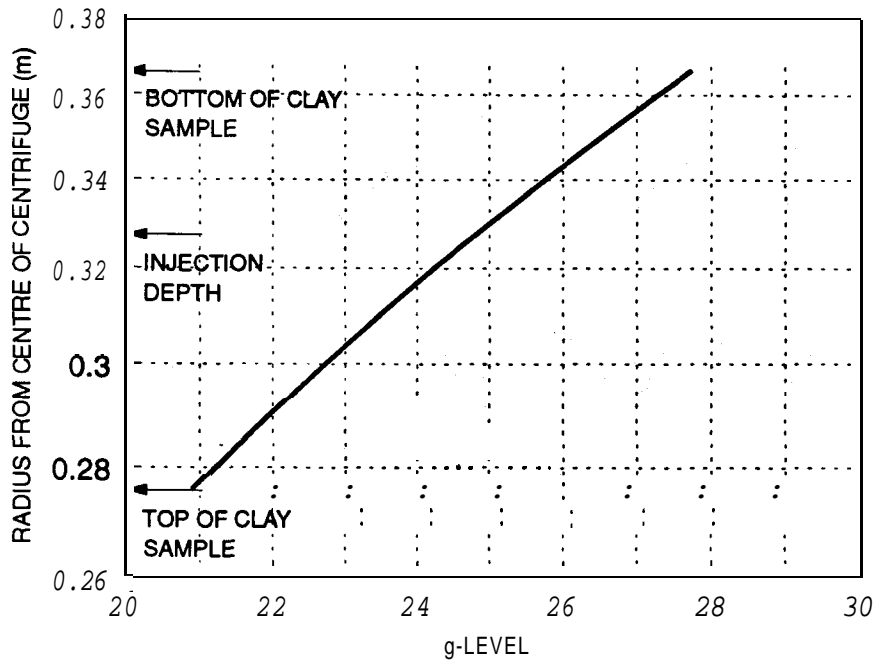


Figure 10: Variation of g-level with depth of **90mm** clay specimen for CYC 10

clay. Figure 9 shows the theoretical stress profiles of the clay at different stages, from prior to centrifuging up to the point before grout injection took place for test⁴ CYC 10. The stresses at depth were obtained by integrating the body forces from the appropriate surface to the depth required as follows :-

$$stress = \rho\omega^2 \int_{r_1}^{r_2} r dr \quad (16)$$

where ρ refers to density, ω refers to angular velocity and $r_{1,2}$ are the radii from the centre of the centrifuge to the appropriate depths. The variation of g-levels with the depth of the clay specimen for test CYC 10 carried out at **260.3rpm** is shown in Figure 10.

5 Testing Procedure

The aim of these series of centrifuge experiments was to observe mechanisms occurring due to the injection of a single phase fluid into clay under varying vertical and horizontal stress conditions. The pre-consolidation pressure was set in the consolidometer. By controlling the rotational speed of the centrifuge and **allowing** equilibrium pore pressure conditions to develop, the OCR and hence K_o of the clay at a specific depth could be determined.

Refer to Table 1, p 12

Test No.	r p m	g-Level ⁵	OCR ⁵	K_o ⁵	Volume Injected (ml)
CYC 8	576.8	121	1.1	0.65	8.08
CYC 6	450.9	74	3.1	1.03	8.69
CYC 10	260.3	24.7	7.2	1.54	7.16

Table 1: Schedule of Tests

The intention was to carry out grouting injections in clay with K_o values ranging from less than unity to greater than unity. This was done to test the postulate in rock mechanics that the plane of hydrofracture **will** occur perpendicular to the direction of least normal stress (**Hubbert & Willis, 1957 [4]**). That is, horizontal hydrofractures occurring when K_o is greater than unity and vertical hydrofractures occurring when K_o is less than unity. The K_o values were obtained by the correlation suggested by Schmidt (1966) [8] for **monotonic swelling**:-

$$K_{o,oc} = K_{o,nc}OCR^\alpha \quad (17)$$

where $K_{o,oc}$ is the coefficient of earth pressure at rest for over-consolidated clays, $K_{o,nc}$ is the coefficient of earth pressure at rest for normally consolidated clays (Jaky, 1944 [5]), OCR is the over-consolidation ratio, defined as σ'_{1max}/σ'_1 , α is $1.2 \sin \phi'_c$ and ϕ'_c was taken as 23° for Speswhite Kaolin (Al **Tabbaa, 1987 [1]**). Table 1 shows the series of centrifuge tests conducted. The grout viscosity of the adhesive used was **100cp at 20°C**.

Following the injection of grout, the block of clay was placed in an oven for 30 minutes at **150°C**. This allowed the Loctite adhesive to set. The block of clay was then cut up to reveal the set adhesive.

6 Observations

Figures 11, 12 and 13 show the set adhesive after cutting up the blocks of clay from tests CYC 8, CYC 6 and CYC 10 respectively. Figure 14 shows cross-sectional details of the set adhesive from test CYC 10. For clay on the dry side of critical (i.e. test CYC 10 with OCR of 7.2) with a K_o of 1.54, horizontal fracturing occurred. The plane of fracturing was perpendicular to the direction of least normal stress. However, when the clay was on the wet side of critical with OCR values approximately 3 or less (i.e. tests CYC 8 with K_o of 0.65 and CYC 6 with K_o of **1.03**), no fracturing occurred. Instead, a cavity expansion mechanism took place.

It is interesting to note that the formation of fractures took place in heavily **over-consolidated** soil on the dry side of critical which would behave in a brittle, strain softening manner. On the other hand, soil on the wet side of critical behaves **like a**

⁵at the level of injection

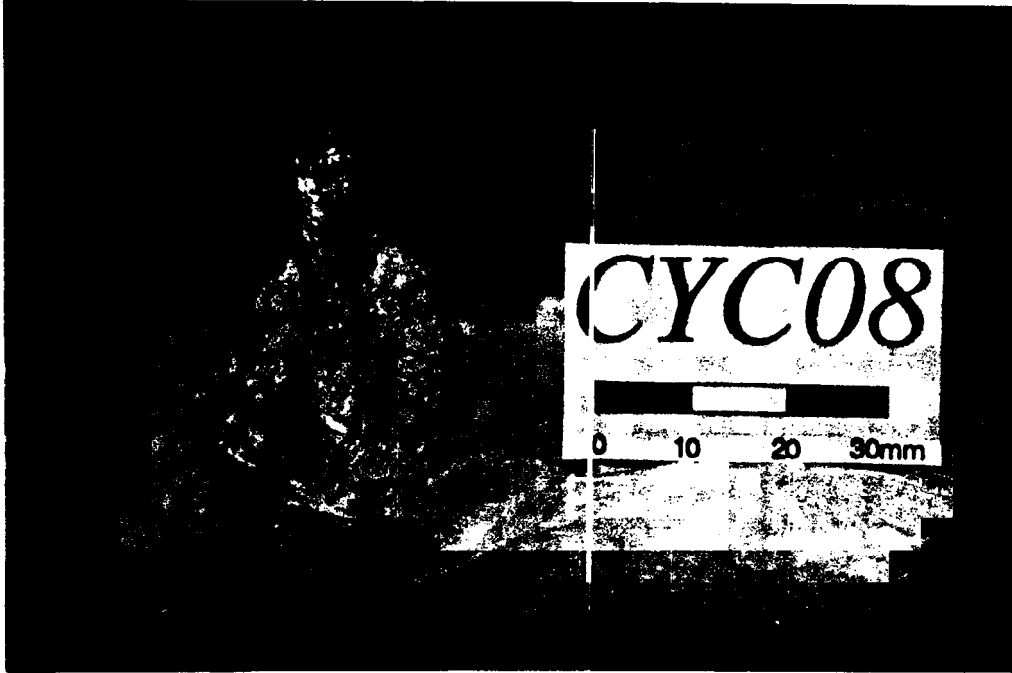


Figure 11: Elevation of Grout ball from Test CYC 8

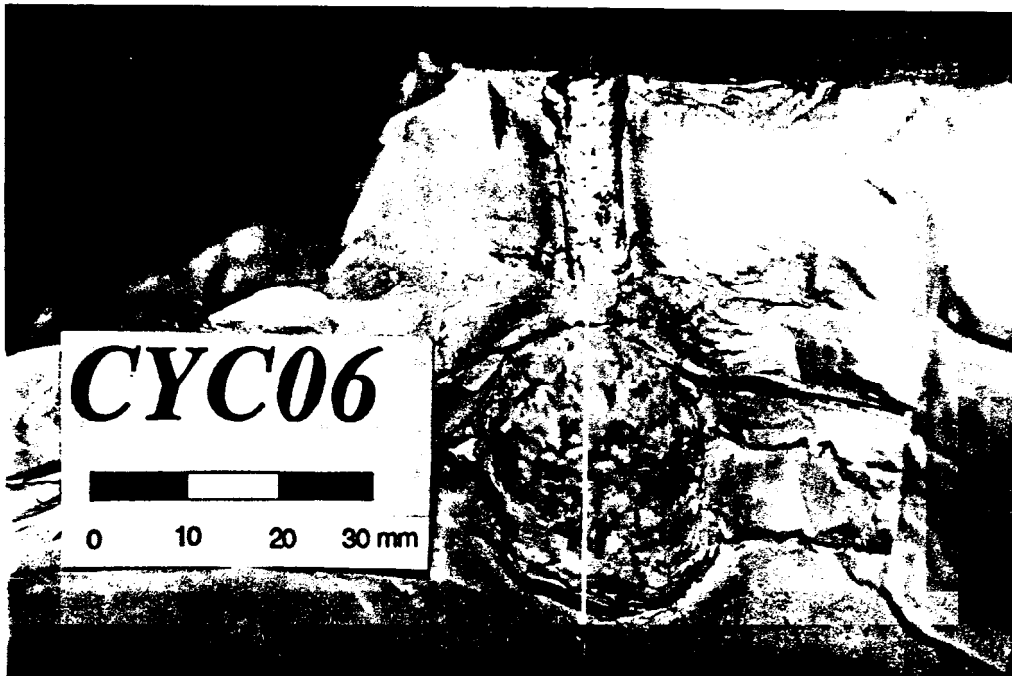


Figure 12: Elevation of Grout ball from Test CYC 6

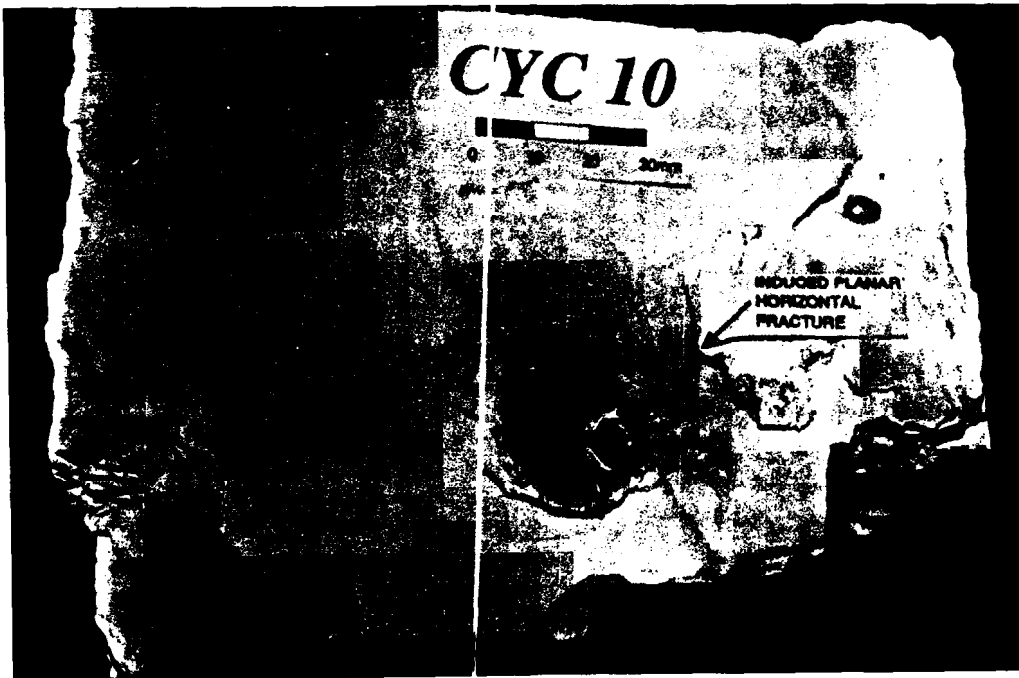


Figure 13: Exposed section of clay on the 'Horizontal' fracture surface in Test CYC 10

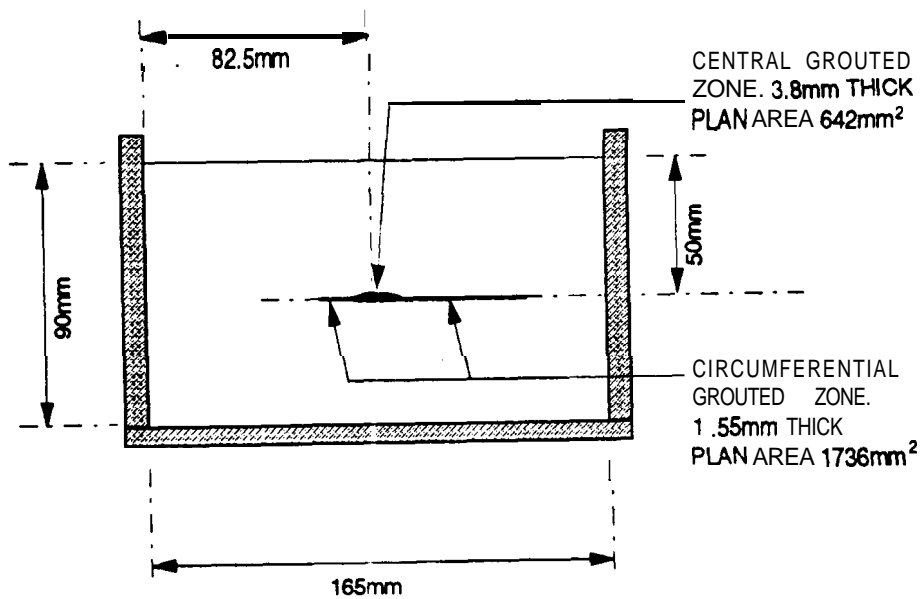


Figure 14: Cross-section of soil model with fracture details from Test CYC 10

ductile material with strain hardening taking place which would explain why fractures did not form. Results obtained from the data acquisition unit are shown in Figures 15, 16 and 17. These account for an air bubble in the syringe during the injection. Pressure loss due to friction between the fluid and both syringe and tubing is negligible and has been neglected.

The typical sequence of events can be seen in Figure 15, for example. The motor was energised at **47.2secs** and pressure builds up in the syringe up to a peak of 628kPa at **47.7secs**. During this time, the **ball** remains fixed in the nozzle and there are no external indications of injection taking place. With the piston continuing to displace, the **ball** was expelled and the injection began creating heave at the soil surface and inducing pore pressures in the nearby clay. The injection continued for 2 seconds with a near constant pressure of 280kPa and an average rate of injection of **3.5ml/sec**. At **49.8secs**, the piston reached the end of its travel. A small amount of further injection was driven by the expansion of a small bubble of trapped air. The final ground heave of **0.78mm** in model CYC 8 would correspond to 81mm at prototype scale.

The mini-drum centrifuge has been most useful for investigating mechanisms in grouting. It has **allowed** a rapid development of grouting equipment and provided an insight to the hydrofracture mechanism. More information about surface and body displacements together with pore pressure changes in the soil would now be beneficial to continue with this research into the fundamental behaviour of hydrofracturing in soils. For this purpose, centrifuge work using the **10m** beam centrifuge will be carried out.

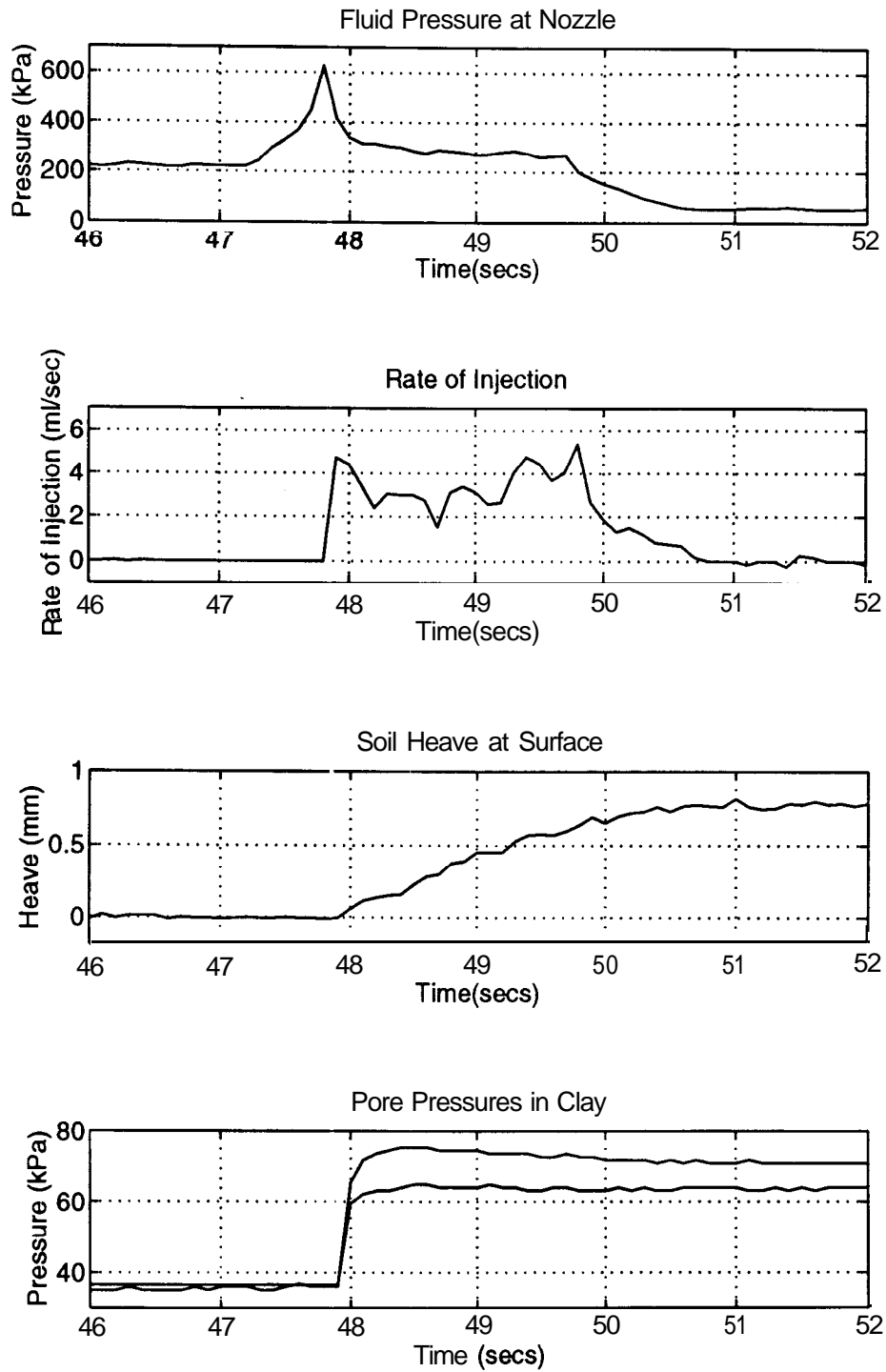


Figure 15: Results from Test CYC 8

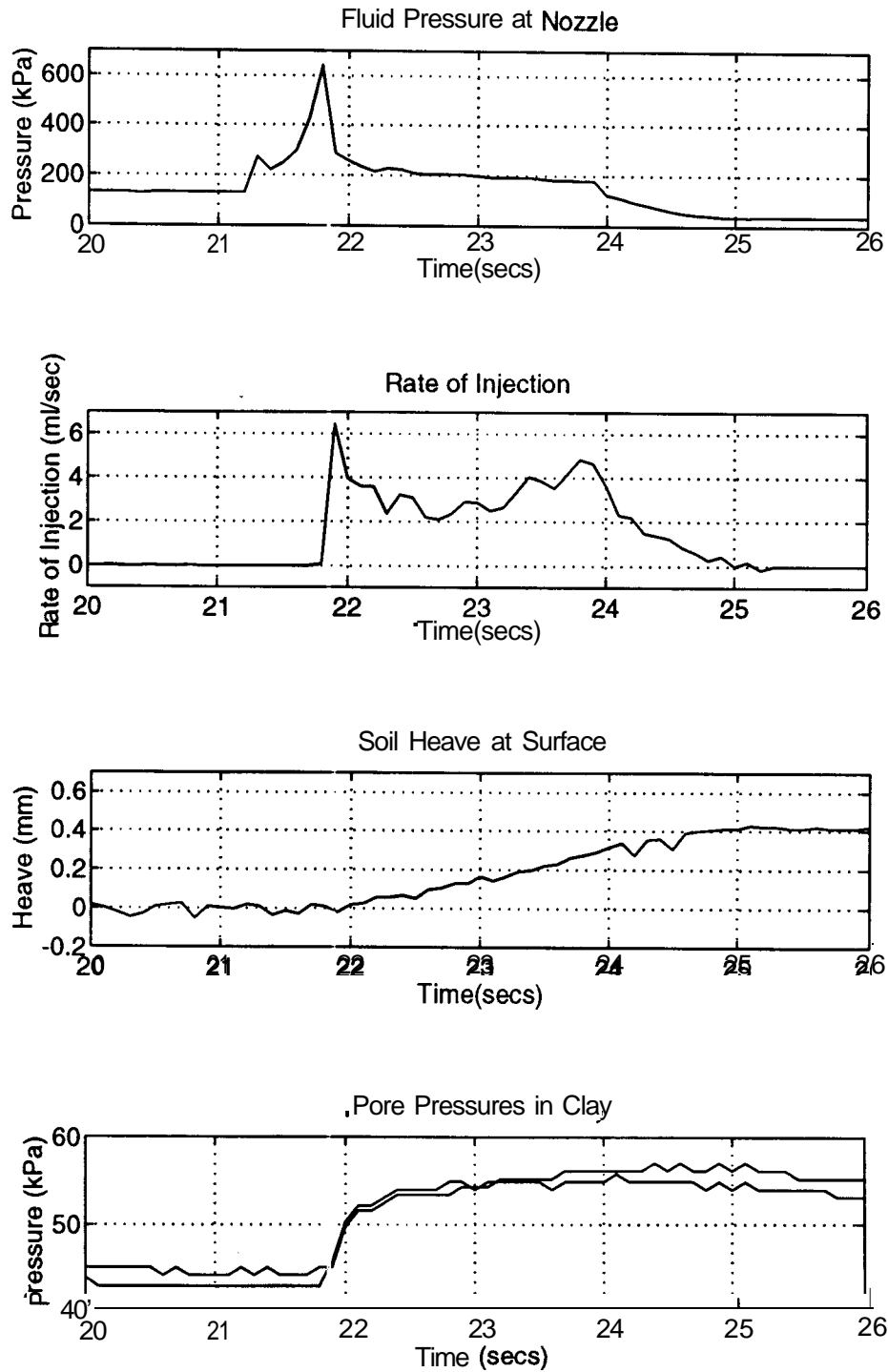


Figure 16: Results from Test CYC 6

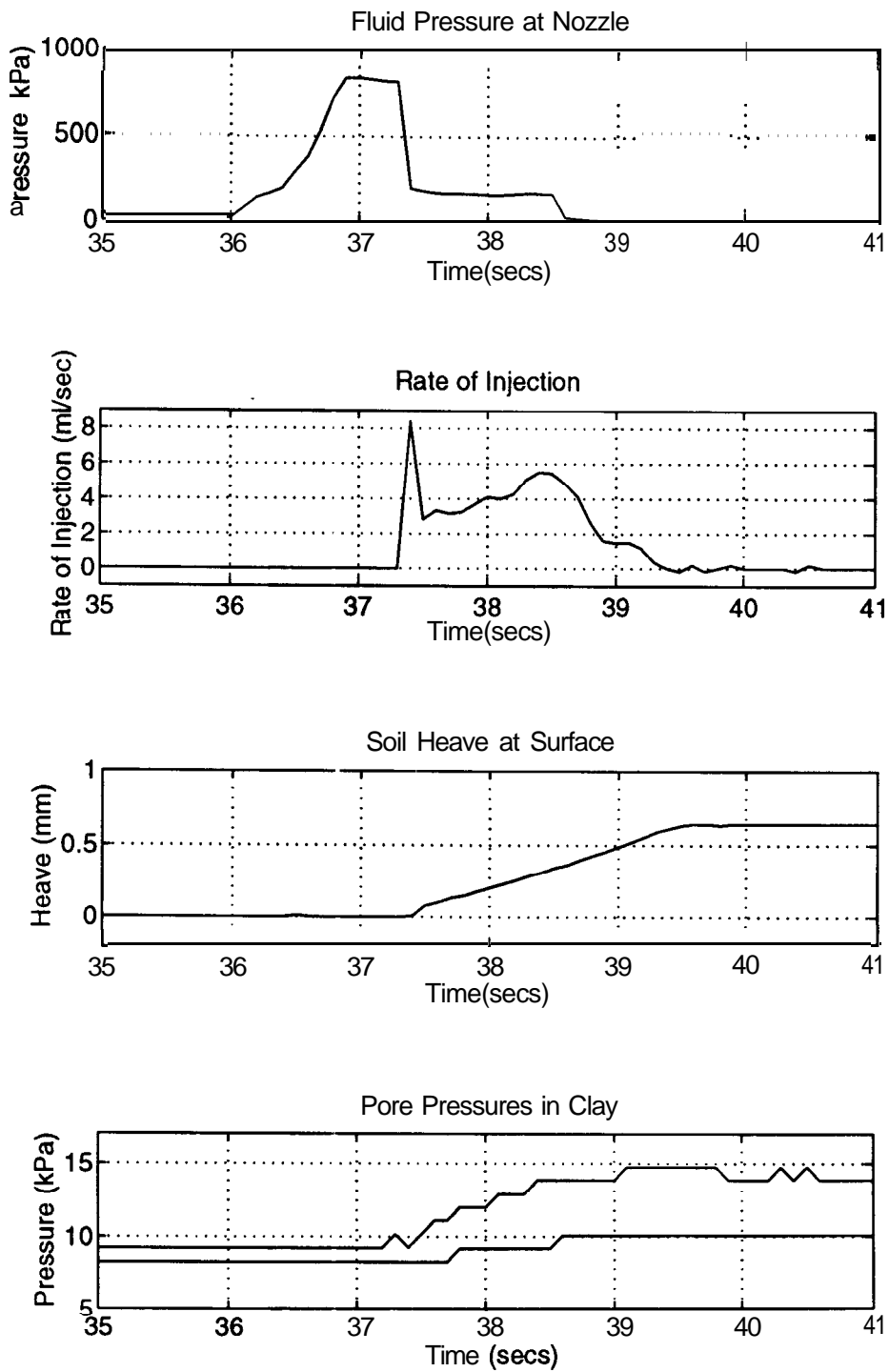


Figure 17: Results from Test CYC 10

Acknowledgements

The assistance of Mr Chris **Collison** in the design and commissioning of the grout injection equipment, of Mr Arthur Timbs, Mr Roy Julian and staff of the Engineering Department Workshop in the manufacture of the equipment, of Mr **Neil** Baker, Mr Stephen Chandler, Mr **Adrain** Brand and Mr Tim Ablett in the arrangements for data **acquisition**, are **gratefully** acknowledged. The authors are grateful to Professor Andrew Schofield for his permission to use the ANS & A mini-drum. This work is funded by a UK SERC-CASE award sponsored by Ove Arup & Partners.

References

- [1] A. Al-Tabbaa. *Permeability and stress-strain response of Speswhite Kaolin*. PhD thesis, University of Cambridge, 1987.
- [2] E.W. Brooker and H.O. Ireland. Earth pressures at rest related to stress history. *Canadian Geotechnical Journal*, 12:1-15, 1965.
- [3] G.H. Foster. *The behaviour of clay in plane strain*. PhD thesis, University of Cambridge, 1977.
- [4] M.K. **Hubbert** and D.G. **Willis**. Mechanics of hydraulic fracturing. *Trans. American Institute of Mining, Metallurgy and Petroleum Engineers*, 210:153-167, 1957.
- [5] J. Jaky. The coefficient of earth pressure at rest. *Journal of Society of Hungarian Architects and Engineers*, pages 355-358, October 1944.
- [6] R.J. **Mair**. *Centrifugal modelling of tunnel construction in soft clay*. PhD thesis, University of Cambridge, 1979.
- [7] V Nadarajah. *Stress-strain properties of lightly overconsolidated clays*. PhD thesis, University of Cambridge, 1973.
- [8] B. **Schmidt**. Discussion of 'Earth pressures at rest related to stress history' by Brooker and Ireland (1965). *Canadian Geotechnical Journal*, 3(4):866-867, 1966.